DOE/NV/03624--0859

Development of an Extruded Plastic Array for Fast Timing

Richard S. Woolf[a*], Bernard F. Phlips[a], Stuart A. Baker[b], Anthony L. Hutcheson[a], Rose Perea[c], David D. Schwellenbach[b], Eric A. Wulf[a]

[a]Space Science Division, U. S. Naval Research Laboratory, 4555 Overlook Ave., SW, Washington, DC, 20375, U.S.
[b]Nevada National Security Site, Transformational Diagnostics and Imaging, Los Alamos, 2900 East Road, Los Alamos, NM, 87544
[c]NRC Research Associate resident at the U.S. Naval Research Laboratory, 4555 Overlook Ave., SW, Washington, DC, 20375, U.S.

*Corresponding Author: richard.woolf@nrl.navy.mil; 202-404-2886

ABSTRACT

This work describes and shows data from a prototype instrument designed to measure fast transient gamma-ray pulses, with potential applications in stockpile stewardship testing. The instrumentation required need to be large, sensitive, low cost, and have the ability to allow for fast transient time sampling at rates of 5 ns, or less. The natural material for an instrument to meet these requirements is an organic scintillator. In order to cover a large area and reduce the overall cost of the detection system (material and electronics), one approach would be to have large pixel elements to build up an array over a few square meters. Unfortunately, this approach will not provide the timing accuracy required for these experiments as large volume scintillation detectors broaden the intrinsic width of the scintillation light pulse due to delays introduced by internal reflections within the scintillator volume. We devised an approach to mitigate these broadening effects from large volume detectors, while remaining at a low cost. Our detectors are a bundle of extruded plastic scintillation bars, readout by wavelength shifting fibers that pipe the scintillation light to a fast light readout device. In this paper we describe the detector unit

and assembly procedure, the fast photomultiplier tube (PMT) and readout electronics, as well as data from the laboratory with a radioactive source and cosmic-ray muons. Additionally, we show results from a detector unit tested at the NRL Mercury pulsed power facility. The concluding section discusses the path forward for this instrument and possible improvements for a field-deployable system.

KEYWORDS

Extruded plastic; organic scintillator; wavelength shifting fibers; photomultiplier tubes

MAIN TEXT

1. Introduction

In stockpile stewardship testing, there exists a need to accurately measure transient gamma-ray sources [1]. A measurement of this nature is difficult for the following reasons: r^{-2} effects resulting from the required displacement between the source and the instrumentation such that one can time delay, and disentangle, the gamma-ray component from the neutron component; and, the ability of the instrumentation to sample the transient at a high frequency (>200 MHz). To make a statistically significant measurement of the source emission, given the large displacement required, one needs instrumentation with large (on the order of square meters) collection area. An approach to address this would be to construct a 2D array (wall) of detectors composed of large pixel elements. In this approach, a large area is populated with relatively few detectors and electronic readout channels, reducing the overall cost and complexity of the instrument. However, large-volume detectors will not adequately sample the timing properties of these transients. To understand why, we first must consider the type of radiation detector used to make this measurement. For a large-volume, high-efficiency, low-cost detector, one should use an organic scintillator (plastic). Scintillating plastics emit photons in response to stimulation from ionizing radiation, are sensitive ($\boldsymbol{\varepsilon}$ > 50% to gamma rays in the 1 – 10 MeV region), can be cast into large (>m^3) volumes, and, in general, are available at a low cost. Additionally, the intrinsic rise time, decay time and pulse width from the scintillation material are extremely fast (on the order of nanoseconds). In terms of fast scintillation detectors, we also note another material that scintillates (via Cherenkov emission) is lead glass. The scintillation mechanisms for this material are extremely fast, on the order of 100 ps. However, while this material is fast and sensitive to gamma rays, the main drawback is its intrinsic low light yield, roughly three orders of magnitude lower than that of plastic scintillator.

The light from these materials is read out by a sensor, such as a photomultiplier tube (PMT) or a silicon photomultiplier (SiPM). A PMT sensor, for instance, is characterized by its rise time, transit time, and transit time spread in response to stimulation by light from a scintillator. The response of a PMT is directly related to its size as smaller PMTs yield faster response times. The converse is also true. In order to minimize the time response contributed by the PMT, one should use a small (A_{eff} of the photocathode ~10 mm^2) PMT. Thus, the overall response of the measured signal is a convolution of the intrinsic timing characteristics of the scintillation material and the light readout device.

2. Motivation

The work discussed within, motivated by [1], requires sampling the timing profile of the transient events on the order of 5 ns (or less). At first glance, this requirement would appear to be trivial given that many nuclear and particle physics experiments routinely perform timing experiments with sub-nanosecond resolution [2]. However, most experiments are concerned about timing the rise of a pulse and are not affected much by the width of the pulse, as long as the detector recovers before the next event. Because timing a pulse can easily be achieved to $1/10^{\text{th}}$ the rise time of a pulse, sub-nanosecond timing is relatively easy with 5 ns rise time pulses. For this experiment, the transit time and transit time spread are not very important, but the width of the pulse is important.

In a previous experimental campaign we investigated how the volume, as well as reflective material and surface treatment, affected the width of a scintillation light pulse. The scintillating materials used in this study were Eljen (EJ) plastics EJ-200, EJ-204, and EJ-228, and Schott lead glass (SF56A). The detector volume ranged from 4.6×10^1 cm^3 (0.75″ × 0.75″ × 0.5″) to 1.7×10^4 cm^3 (16″ × 16″ × 4″). We additionally investigated how much the pulse width could be reduced by eliminating reflections via the implementation of black cardboard and black spray paint on the surfaces, as opposed to white diffuse reflector.

We found that the effect of size and shape on the pulse width is due to multiple reflections of the light before being collected in the PMT. These reflections are typically considered beneficial because they enhance the light collection and provide a more homogeneous response throughout the scintillator. This improves the energy resolution and is the reason most scintillators have surfaces and wrappers designed to maximize reflections. For fast timing experiments, however, these reflections aid in broadening the width of the scintillation pulse. In Figure 1, we summarize our results for the various-sized EJ-200 samples, with different reflective surfaces, EJ-204, EJ-228, and SF56A vs. time response. Under irradiation from cosmic-ray muons, we found that the time response varied between 2.9 ns (4.6×10^1 cm^3) and 33 ns (1.7×10^4 cm^3). Based on these results we determined that small volume scintillation detectors (less than one liter), with fast readout devices, would be needed to achieve 5 ns (or less) sampling resolution.

Thus, in order to cover a large area and achieve a fast time response, many segmented and optically isolated small detector elements, read out by fast devices, are needed. However, using many, small independent devices would lead to prohibitive cost in terms of channel count, materials and readout devices. In the next section we discuss our approach to mitigate the costs of using many small detector elements while achieving the fast time response.

3. Instrumentation

3.1 Approach

We have designed and preliminarily tested detector units to measure narrow time-width pulses. The detector concept consists of a bundled array of extruded plastic scintillation bars, with wavelength shifting (WLS) fibers inserted into the extruded holes, which then pipe the scintillation light onto a small, fast PMT. Extruded plastic scintillator technology is used in high-energy physics experiments (e.g., MINOS [3] and Minerva [4]) that require a large volume of scintillation material at a reduced cost. To extrude plastic scintillator, the process involves properly mixing the raw materials that compose the final scintillator (polystyrene pellets and dopants), feeding the mixed materials through a puller at a specific rate, all at a given temperature and pressure within a vacuum tank. The mixed material is then fed through an extruder, which then passes through a melt pump and a die [5]. The dies can have custom shapes, depending on the needs of the experiment, all of which contain the extruded hole(s). [6] shows examples of extruded plastics that have triangular, hexagonal and rectangular shapes. To improve light collection, and provide optically isolated units, external reflective cladding is applied to the outside of the extruded plastic.

A detector unit consists of twenty-five 1 cm × 1 cm × 20 cm extruded plastic scintillation bars, with 1.5-mm-diameter holes in each bar (Figure 2). The material has the following composition: polystyrene + 1% 2,5-Diphenyloxazole (PPO) + 0.03% 1,4-bis(5-phenyloxazol) benzene (POPOP). The scintillator peak emission wavelength is ~420 nm and the scintillation decay time is ~3 ns [7]. See Figure 3 for the emission and transmission properties of this material.

A WLS fiber is inserted into the bar to pipe the scintillation light down its length via total internal reflection. The WLS fibers are manufactured by Bicron (BCF-92) [8]. The diameter of each WLS fiber is 1.2 mm. The extruded plastic bars are assembled into a tightly packed 5 × 5 array, and all 25 WLS fibers are ganged together and coupled to a small, fast PMT. Each scintillation bar was extruded with external white cladding (15% TiO_2 in polystyrene [7]) on the four long (1 cm × 20 cm) faces. Within the extruded hole, there is an air gap coupling the WLS fiber to the scintillator. While direct coupling via optical grease or epoxy would yield improved light collection, for the sake of simplicity and reproducibility and because the scintillator light yield is high, we designed the detector unit to have an air gap between the scintillator and the WLS fiber.

Additionally, to better understand how the number of fibers in the bundled array affects the overall time response, we constructed two test arrays with only one extruded plastic plus fiber and five extruded plastics plus fibers, readout by a fast PMT.

3.2 Assembly

For housing of the extruded scintillation bars plus fibers, we needed an approach that would: 1) have the entire bundle enclosed in a light tight assembly, 2) have a reflective surface at the interface where the fibers exit the bars, and 3) allow for the fibers to be guided onto the PMT window. We accomplished the first item by encasing the detector components within 3D-printed parts that includes: the 5 cm × 5 cm × 20 cm housing for the extruded bars, a truncated pyramid that interfaces the housing for the bars with the housing for the PMT, and a PMT end cap. For the second item, we placed a layer of VM2000 specular reflector [10] at the interface of the truncated pyramid and the extruded plastic bars to allow for any light generated near the ends of a bar to be reflected, thus improving the overall light collection. To meet the criteria of the third item, inside the truncated pyramid the fibers pass through an intermediate plane halfway up, acting as a guide to the pyramid's apex, where they exit and are bundled prior to interfacing with a PMT.

Figures 4–8 shows the process of assembly for a single detector unit. The truncated pyramid has the 25 fibers fed through the bottom end, where they are guided through the intermediate plane and exit through the top of the pyramid. After exiting, the fiber ends are tightly bundled and molded into a tip. The mold is a transparent epoxy, which, after curing, is sanded to yield a smooth surface that can interface with the PMT window. The optical coupling between the molded tip and the PMT window is a 1-mm-thick silicone pad (Eljen 560 [11]).

On the other end (facing up in Figure 4), the extruded scintillator bars (Figure 5) are placed over the fibers. The bundled bars, with fibers in place, are then loaded into the scintillator bar housing. The truncated pyramid and scintillator bar housing are bolted together through interfacing flanges. Figure 6 shows the near complete configuration with the pyramid separated from the bar housing to show the path of the fibers. Figure 7 shows the same configuration under dark conditions, illuminated by a UV light, clearly demonstrating the light in the WLS fibers being guided to the end where the PMT would be located. The PMT (see section 3.3) is inserted into a recessed holder on top side of the truncated pyramid, then covered with an end cap. The end cap has a small hole on the back side to allow the signal and high-voltage cables to pass through and interface with the data acquisition system and high-voltage power supply. Figure 8 shows a fully assembled detector unit.

3.3 Readout

One aspect of this work was to performance test two very fast PMTs as potential light readout devices. The PMTs we used in this experiment are manufactured by Hamamatsu, model nos. R7600U and R9880U-01. The R7600U has a photocathode with a square geometry and an effective area of 18 mm × 18 mm. The interfacing PMT base is the E5996 and operates the PMT with a negative bias voltage. The maximum bias voltage that can be applied between the anode and cathode is 900V. The R9880U-01 has a circular geometry and an effective area of 8-mm diameter. The interfacing PMT base is the E10679-

02 and operates the PMT with a negative bias voltage. The maximum bias voltage that can be applied between the anode and cathode is 1100V. Each PMT type has the following timing properties: a rise time of 1.6 ns (R7600U) and 0.57 ns (R9880U-01); a transit time of 9.6 ns (R7600U) and 2.2 ns (R9880U-01); and a transit time spread of 0.35 ns (R7600U) and 0.2 ns (R9880U-01) [12][13]. Figures 4–8 show the truncated pyramid that accepts the R9880U-01 PMT. There is also a 3D-printed truncated pyramid (and associated end cap) that accepts the R7600U. The extruded plastic and fiber bundle are the same amongst each type. Lastly, the one fiber plus one plastic and five fibers plus five plastics test arrays are readout by the R9880U-01.

The PMTs are biased by iseg brand high-voltage modules that can supply up to 1.3 mA of current and 2 kV of high voltage [14]. The PMT signals are digitized using flash analog-to-digital converters (fADCs). We tested two types of fADCs, both manufactured by Struck Innovative Systeme (SIS), model nos: 3316 and 3305 [15][16]. The SIS3316 is a 16-channel, VME-based 14-bit, 250 MHz digitizer. Each channel is self-triggered and has the ability to record the raw trace in oscilloscope mode for post-processing and subsequent analysis. To achieve higher sampling rate, we used the SIS3305 units. The SIS3305 is an 8-channel VME-based 10-bit, 1.25 GHz digitizer. Each channel has an input range of ±1 V and software adjustable trigger threshold for rising or falling edge. The SIS3305 saves a software adjustable number of samples before the trigger and after the trigger to allow the initial baseline and entire pulse to be recorded. The maximum number of samples per trigger—in the selected operated mode—is 3072 (or 2457.6 ns). The module can also run at 2.5 GHz and 5 GHz with either four or two channels enabled, respectively. Multiple modules can be chained together sharing a common clock and common start signals. An external trigger/timing signal can be supplied to the module and a time-to-analog converter will measure the time between the external signal and internal triggers to an accuracy of 27 ps. Both SIS modules are powered by a VME crate with a VME single-board-computer running Ubuntu Linux for data acquisition, data analysis, and streaming the data to disk.

4. Results

4.1 Laboratory Testing

We have assembled a 4×4 array of detector units, which include seven (25-fiber), one (one-fiber), and one (five-fiber) units, readout by the R9880U-01 PMT; and seven (25-fiber) units readout by the R7600U PMT. The 16 units are held in an aluminum frame (Figure 9) and readout by two SIS3305 units and a 32-channel iseg brand power supply. We tested each unit in the laboratory by irradiation via a radioactive check source and cosmic-ray muons. Laboratory sources provide known energy deposits in the scintillator that one can use to calibrate a detector unit. The radioactive source used was a set of thoriated welding rods, which primarily emits 2.614 MeV photons, resulting in a Compton edge energy deposit in the plastic scintillator of 2.214 MeV. The rods are typically from 1% to 2% thorium oxide, have a diameter of 2.4 mm, length of 15 cm, and contain 0.23 grams of thorium [17].

Cosmic-ray muons are minimum ionizing particles (MIPs) that deposit their energy proportionally along the path of ionization through the detector volume. The background rate for cosmic-ray muons is, on average, ~1 cm^{-2} $minute^{-1}$. The direction of the maximum flux from muons is towards zenith and falls off as the $\cos^n(\Theta)$ where $n \sim 2$ and Θ increases towards the horizon. A muon passing through the detector unit will lose energy while traversing matter according to the Bethe-Bloch formula [18], with a *dE*/*dx* for a muons of ~1.8 MeV cm^2/g. Thus, for a muon passing through 1-cm-thick plastic scintillator ($\boldsymbol{\rho}$ = 1.0 g/cm^3), the energy deposited will be ~1.8 MeV. Muons passing through the entire width of the detector will result in an energy deposit that is, on average, ~10 MeV. For MIPs, as well as other charged particles, these events will produce Landau-distributed spectra when traversing the scintillation material [19].

For data acquisition, we typically bias the PMTs between 700 and 900V and collect 1×10^4 triggered events for each detector unit with the SIS3305, storing the waveform data for each event. Figure 10 shows a representative PMT pulse from the fiber bundle array, read out by the R9880U-01 PMT, in response to a cosmic-ray muon. We integrate each pulse over a predefined 55 ns window. This integration window encapsulates the full pulse produced by the PMT and accounts for pulses that do not trigger at the same t_0. The integral value from each waveform is tabulated and used to construct a spectral distribution of events. Figure 11 shows a representative spectral distribution produced by a 25 plastic plus fiber bundle array read out by the R9880U-01 PMT. To determine the time response of the detector unit, we select between a lower and upper bound of the source and fit each pulse with a function of

$$f = A\left(\frac{\lambda}{2}e^{\frac{\lambda}{2}(2\mu+\lambda\sigma^2-2x)}erfc\left(\frac{\mu+\lambda\sigma^2-x}{\sqrt{2}\sigma}\right)\right)$$

where *erfc* is the complementary error function, σ is the standard deviation, μ is the mean, λ is the exponential rate (where $\lambda > 0$ and for $\lambda >> \sigma$, the distribution approaches a Gaussian) and A is the amplitude. Determining these parameters for each fitted pulse allowed us to assess the timing performance of an individual detector unit. Figure 12 shows the timing distribution from a detector unit readout by a R9880U-01. We assess the performance of each unit in terms of the mean of the distribution, as determined by a Gaussian fit, which represents the peak FWHM of scintillation pulses measured by a given detector unit.

Based on the muon data, the 25-fiber bundle readout by the R9880U-01 demonstrated a mean in the peak FWHM of 6.5±1.1, while the 25-fiber bundle readout by the R7600U demonstrated a mean in the peak FWHM of 8.2±1.0. The one-fiber and five-fiber bundle, both readout by the R9880U-01, demonstrated a mean in the peak FWHM of 1.2±0.4 and 5.4±1.5, respectively.

As noted earlier, we performed a series of runs using a radioactive laboratory source (thoriated welding rods). At the nominal bias voltage used for the muon runs we found a peak clearly distinguished from background/noise. For the runs with the thoriated rods, we raised the gain on the PMT to near the maximum allowed based on the specifications in the data sheet. This allowed for the detectors to clearly distinguish the source from the background/noise component. The performance of plastic scintillation detectors in response to gamma rays with energies of >100 keV will not yield a photopeak in the spectrum resulting from full absorption of the gamma ray, as is the case in most inorganic scintillation detectors. Instead the spectrum will show the Compton edge energy and the low-energy continuum below the edge. Assessing where the maximum energy deposited on the Compton edge has been investigated previously finding that it is dependent on the size and shape of the scintillator volume [20]. The method we used to assess the location of the Compton edge, and hence perform the timing analysis for a given detector, involved choosing a location that lies 20% below the Compton edge maximum height and integrating over a fixed region around that location. The runs with the thoriated rods demonstrated an improved timing performance for both the circular and square geometry PMTs. The circular PMTs observed a reduction in the mean of the peak FWHM by, on average, 1.5 ns, while the square PMT observed a reduction of, on average, 0.8 ns.

4.2 Pulsed Power Facility

To test the performance of the prototype detector unit irradiated by a bright, fast transient, we exposed the unit to source of bremsstrahlung X-rays at the NRL Mercury facility. Mercury is a pulsed-power machine that provides a pulse of ~150 kA of electrons at up to 6 MV, producing a terawatt of beam power for tens of nanoseconds [21]. While the nature of a Mercury transient impulse event (50 ns, FWHM) is an order of magnitude slower than what is specified for the timing performance of these detector units, testing at this facility provided a fast and bright signal for testing, allowing us to understand the response to a relatively fast transient.

We placed the detector unit at a vantage point of 12 m behind the front end of the Mercury machine, the largest standoff achievable at the facility. Previous studies with scintillation detectors at Mercury demonstrated the harsh environment detectors encountered, leading to long periods of PMT dead time. We used the R9880U-01 PMT and applied a negative bias of 475 V, which was the reduced setting we chose after initial tests at higher voltages showed saturation. We read out the unit using the SIS3316 (4 ns sampling rate) fADC. Figure 13 shows the results obtained by the 25-fiber bundle detector unit in response to the pulsed power shot. The width of the measured pulse by the detector unit is the native width of the Mercury pulse. For comparison, the orange curve shows the signal from a 5 cm × 5 cm × 10 cm lead glass detector readout by the R9880U-01, positioned closer to the front of the machine (~9 m away). Because of the fast time response of lead glass (0.1 ns), the width of the measured pulse is representative of the characteristic profile of the Mercury beam. Comparing the two curves, one can see that the 25-fiber bundle detector has the same time width as the fast lead glass detector. Note the slight offset between the curves is an artifact of time aligning when each detector triggers.

5. Future Work and Discussion

The results obtained through laboratory tests and at the Mercury pulsed power facility are encouraging. Through these tests we have demonstrated the ability to measure multi-MeV energy deposits in the extruded plastic scintillator with a pulse FWHM of ~6 ns for muons (~10 MeV), and <5 ns for the thoriated rods (~2 MeV). For the runs with thoriated rods, we increased the bias voltage on the PMT, compared to the muon runs, to be able to cleanly observe the Compton edge features in the spectral distribution above the lower-energy background/noise components. For specific applications, such as those encountered in the Mercury environment (intense bremsstrahlung beam with ~6 MeV endpoint) or at other facilities, we will investigate how the timing performance is affected as a function of bias voltage in order to optimize the detector timing performance while avoiding saturation and overflow of the PMT and fADC data acquisition, respectively. Additionally, from these tests, we learned that the fiber bundles readout by the circular PMT (R9880U-01) consistently outperformed comparable bundles readout by the square PMT (R7600U). Future instrumentation would likely baseline the R9880U-01 PMT.

For an instrument array in an operational scenario, the frontal area required would be 9 m^2 (3 m × 3 m). Building an instrument based on the detectors outlined in this work would thus require ~1850 units and the same number of electronics and high-voltage channels. For such a large array, it would be prudent to have a larger pixel size to reduce the number of channels. For a deployable instrument with more modest channel count, additional future work will investigate the performance of custom extruded plastics with a larger cross section (4 cm × 4 cm) and with the same diameter (1.5 mm) extruded hole. In this design, one pixel would comprise 25 extruded scintillation bars plus fibers, with a total cross-sectional area of 20 cm × 20 cm. By taking the mounting flange into account, the pitch between adjacent detectors would be ~25 cm. Thus, by using pixels with larger cross-section extruded plastics, a full instrument with 9 m^2 of frontal area would require 144 detectors (12×12 array) and associated electronics and high-voltage channels. Our group has a precedence for building [22] and deploying [23][24] large-area detector arrays of this magnitude for gamma-ray and fast neutron detection. Additionally, it would be beneficial to investigate increasing the number of extruded plastics plus fibers comprising one pixel from a 5×5 array to 6×6 array. If we are able to fit all 36 fibers onto the small PMT window and achieve comparable timing performance, then the needed number of channels would be further reduced by 30%.

Acknowledgments

This work was sponsored by Office of Naval Research 6.1. We would like to thank the NRL Space Science Division electronics technician, Mary Rambert-Johnson for assembly of the detector units discussed in this work, as well as W. Neil Johnson for his part in developing the analysis routines. We also thank undergraduate students Emily Kong and Mehmet Esat Kilinc for their assistance on this project. Their participation was made possible, in part, via the Naval Research Enterprise Internship Program (NREIP). Lastly, we thank our NRL Plasma Physics collaborators for access to the Mercury Pulsed Power facility. Portions of this work were supported by Mission Support and Test Services, LLC, under Contract No. DE-NA0003624 with the U.S. Department of Energy, National Nuclear Security Administration, NA-10 USDOE NA Office of Defense Programs (NA-10) and by Site-Directed Research and Development Program. DOE/NV/03624—0859.

References

[1] E. Hutterer, *1663 – the Los Alamos Science and Technology Magazine* (October 2017) 18.

[2] P. H. Regan, *Appl. Rad. Iso.* 70 (2012) 1125.

[3] A. Pla-Dalmau, et al., *IX Int. Conf. Cal. Part. Phys.* (2001) 513.

[4] A. Pla-Dalmau, et al., *IEEE NSS-MIC Conf. Rec.* (2005) 1298.

[5] A. Pla-Dalmau, et al., *IEEE NSS-MIC Conf. Rec*. (2003) 102.

[6] D. Beznosko, et al., *IEEE NSS-MIC Conf. Rec.* (2004), 1.

[7] A. Pla-Dalmau, in *private communications,* email, 22 June 2020.

[8] St. Gobain Crystals, BCF-92, https://www.crystals.saint-gobain.com/products/scintillating-fiber

[9] Stratasys Direct, https://www.stratasysdirect.com

[10] 3M Vikuiti Enhanced Specular Reflector (ESR), https://www.digikey.com/en/pdf/3/3m/3m-vikuiti-enhanced-specular-reflector-esr.

[11] Eljen Technology, EJ-560, https://eljentechnology.com/products/accessories/ej-560.

[12] Hamamatsu Photonics, R7600U, https://www.hamamatsu.com/resources/pdf/etd/R7600U_TPMH1317E.pdf.

[13] Hamamatsu Photonics, R9880U-01, https://www.hamamatsu.com/resources/pdf/etd/R9880U_TPMH1321E.pdf.

[14] ISEG Germany, EDS, https://iseg-hv.com/en/products/index#collapse_EDS.

[15] SIS3316, 16 channel, VME digitizer, https://www.struck.de/sis3316.html.

[16] SIS3305, 8 channel VME digitizer, https://www.struck.de/sis3305.html.

[17] Thorium Containing Welding Rods (1990s) https://www.orau.org/ptp/collection/consumer%20products/weldingrod.htm

[18] C. Amsler, et al., *Review of Particle Physics. Physics Letters B* 667(1-5) (2008) 1-6.

[19] L. Landau, *J. Phys*. (USSR) 8 (1944) 201.

[20] H. H. Knox, T.G. Miller, *Nucl. Instrum. Methods* 101(3) (1972) 519.

[21] R. J. Allen, et al., *Proc. 15th IEEE Int. Pulsed Power Conf. Proc.* (2005) 318.

[22] R. Woolf, et al., *Nucl. Instr. Methods Res. A* 784 (2015), 398.

[23] L. Mitchell, et al., *IEEE NSS-MIC Conf. Rec.* (2009) 110.

[24] A. Hutcheson, et al., *IEEE Conf. Tech. Homeland Sec*. (2013) 360.

FIGURES

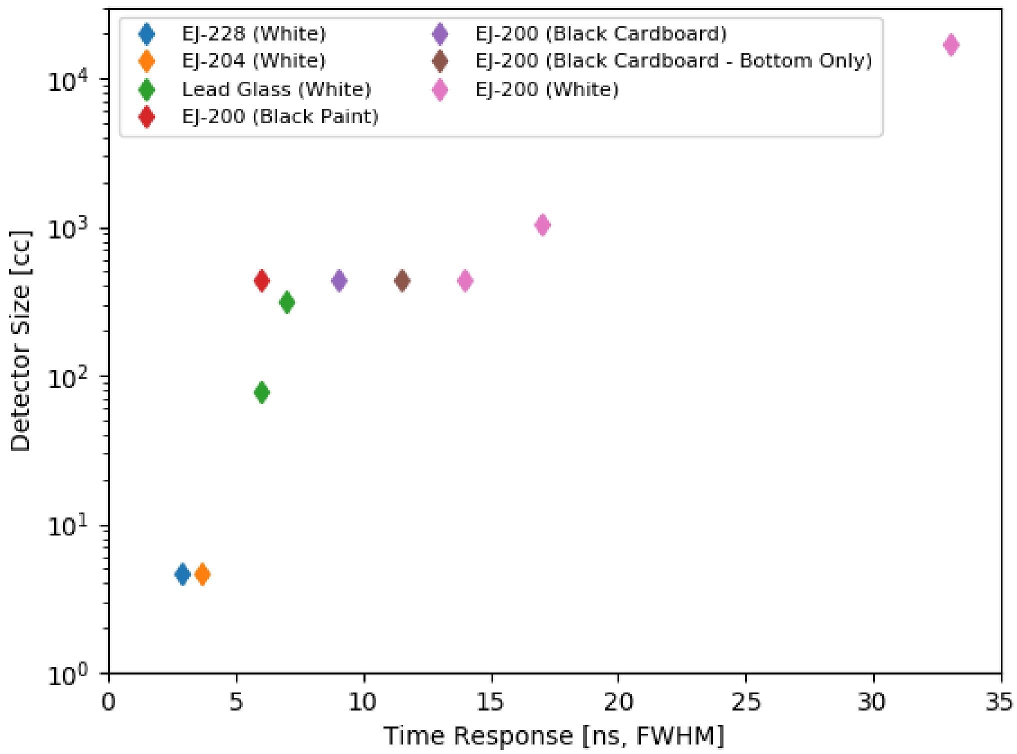

Figure 1: Detector size in cubic cm vs. the time response, in ns (FWHM).

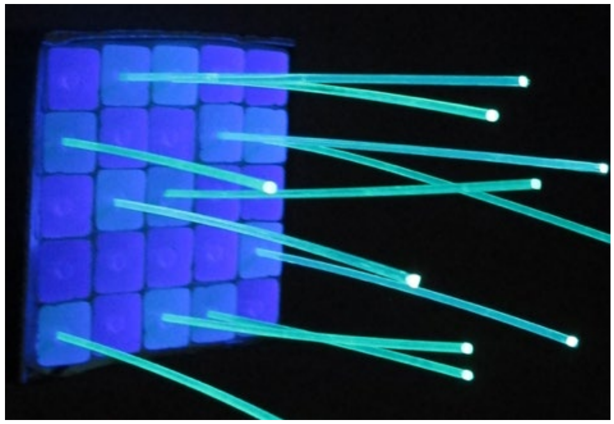

Figure 2: 5×5 array of 1 cm × 1 cm cross-section extruded plastic scintillation rods. Exiting a few of the rods are the 1.2-mm diameter WLS fibers. We show the end of the 25-fiber bundle under illumination by a UV light.

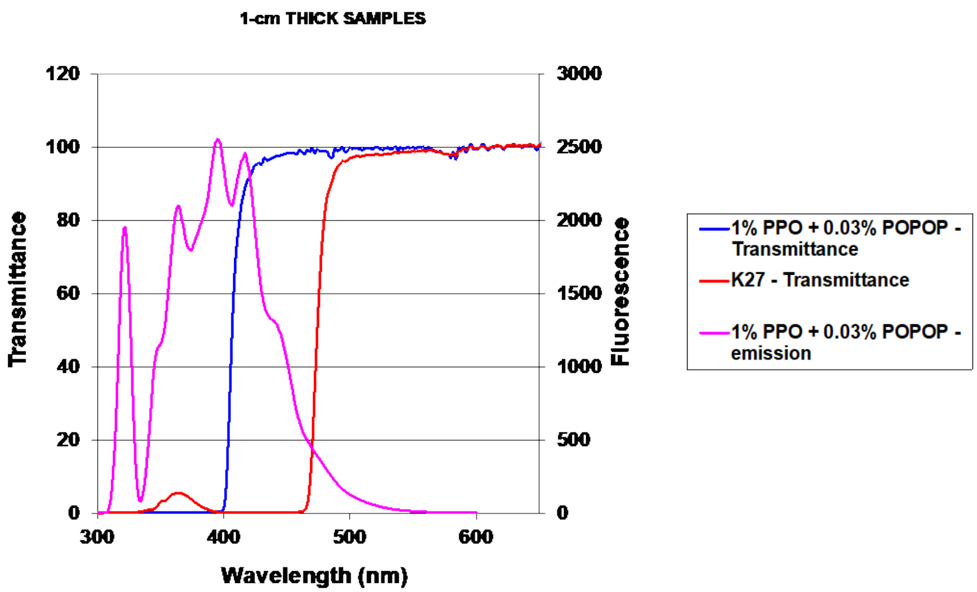

Figure 3: Spectra of the transmittance vs. wavelength for the 1-cm-thick extruded plastic samples.

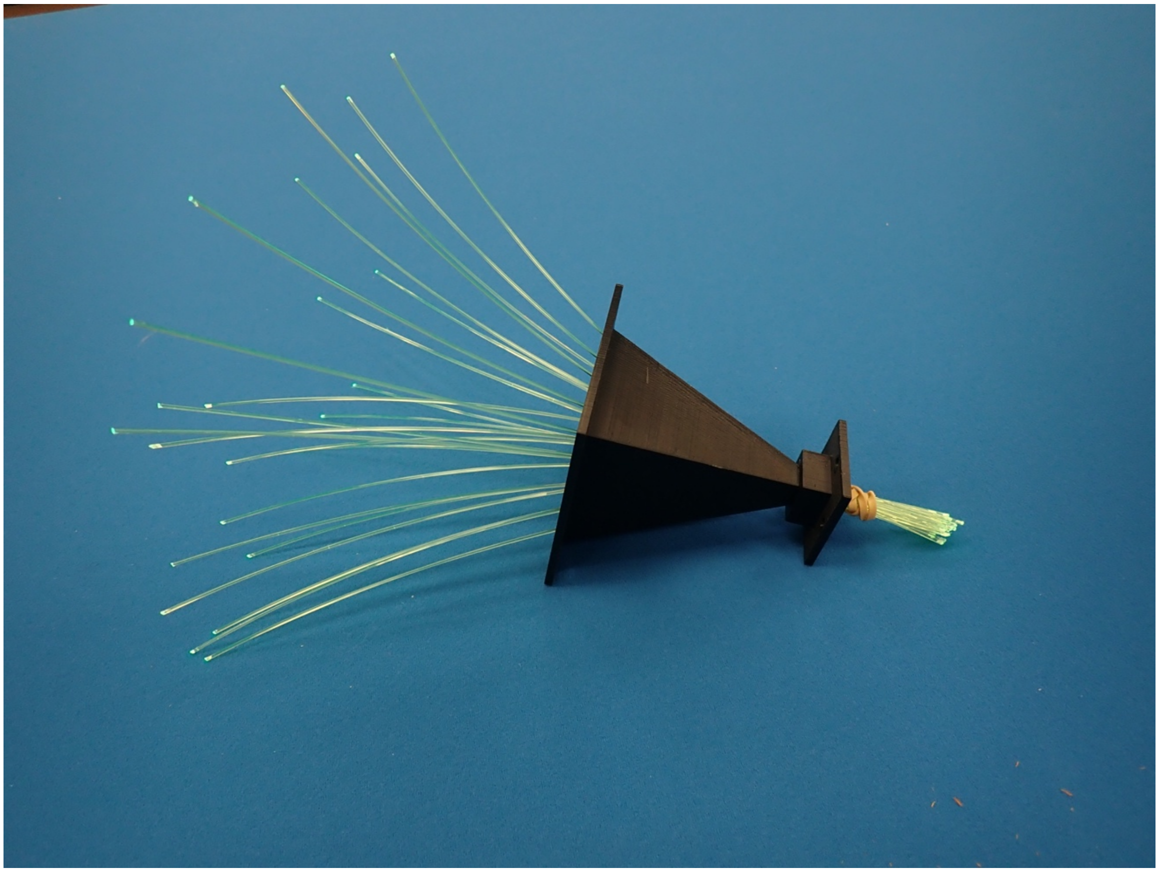

Figure 4: 3D-printed truncated pyramid with 25 equal-length WLS fibers. Inserting the fibers into the pyramid and bundling them with a rubber band on the top side is the first step in the assembly process.

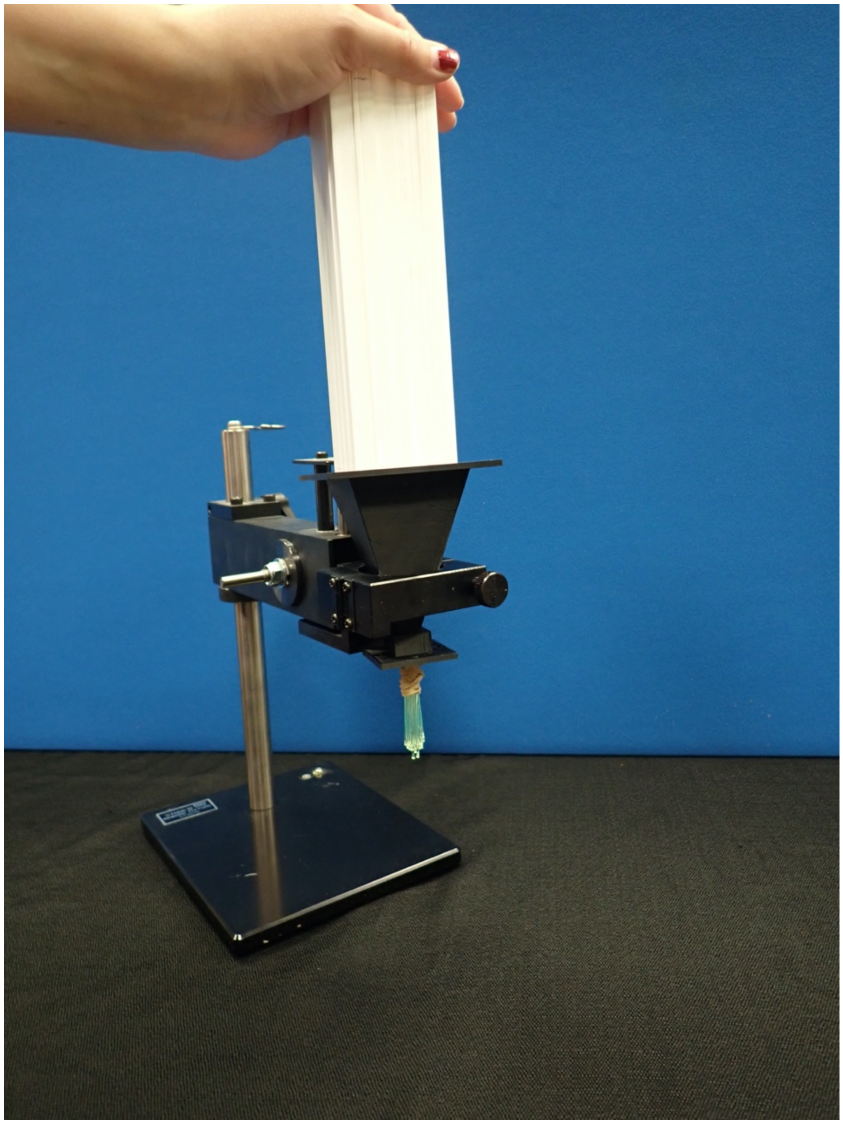

Figure 5: The next step in the assembly process is to invert the pyramid and place it in a holding fixture. Once in place, the extruded bars are placed on fibers and ganged together as shown here.

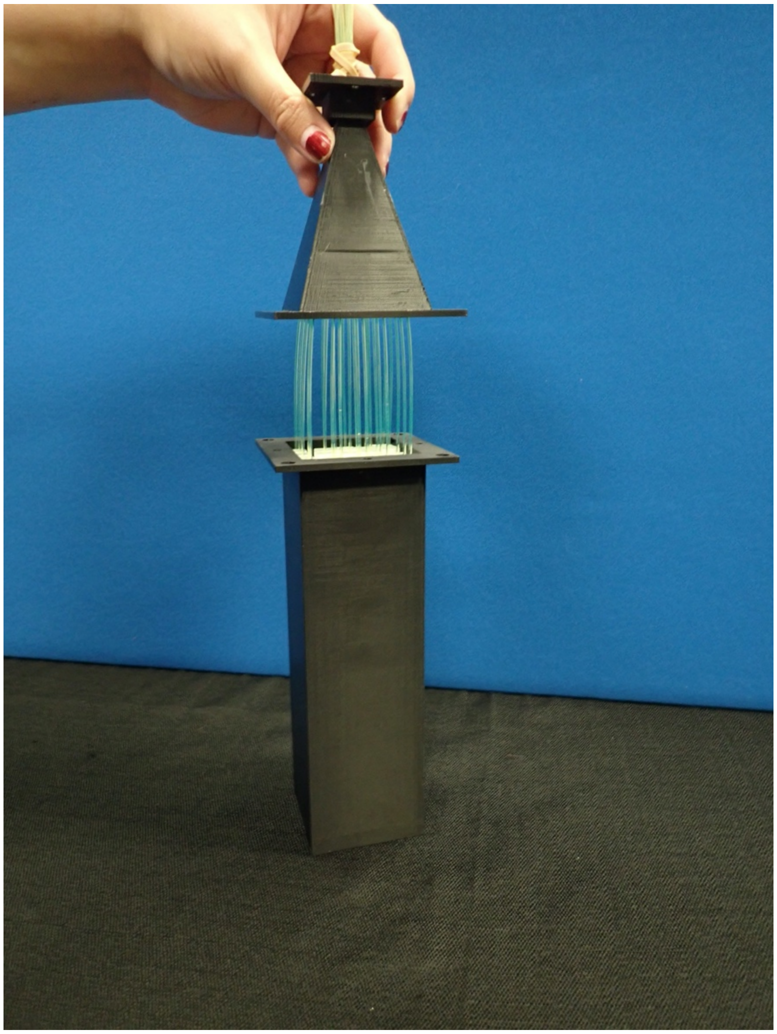

Figure 6: The bars, with fibers in place, are inserted into their housing. This figure shows the process of attaching the pyramid to the bar housing.

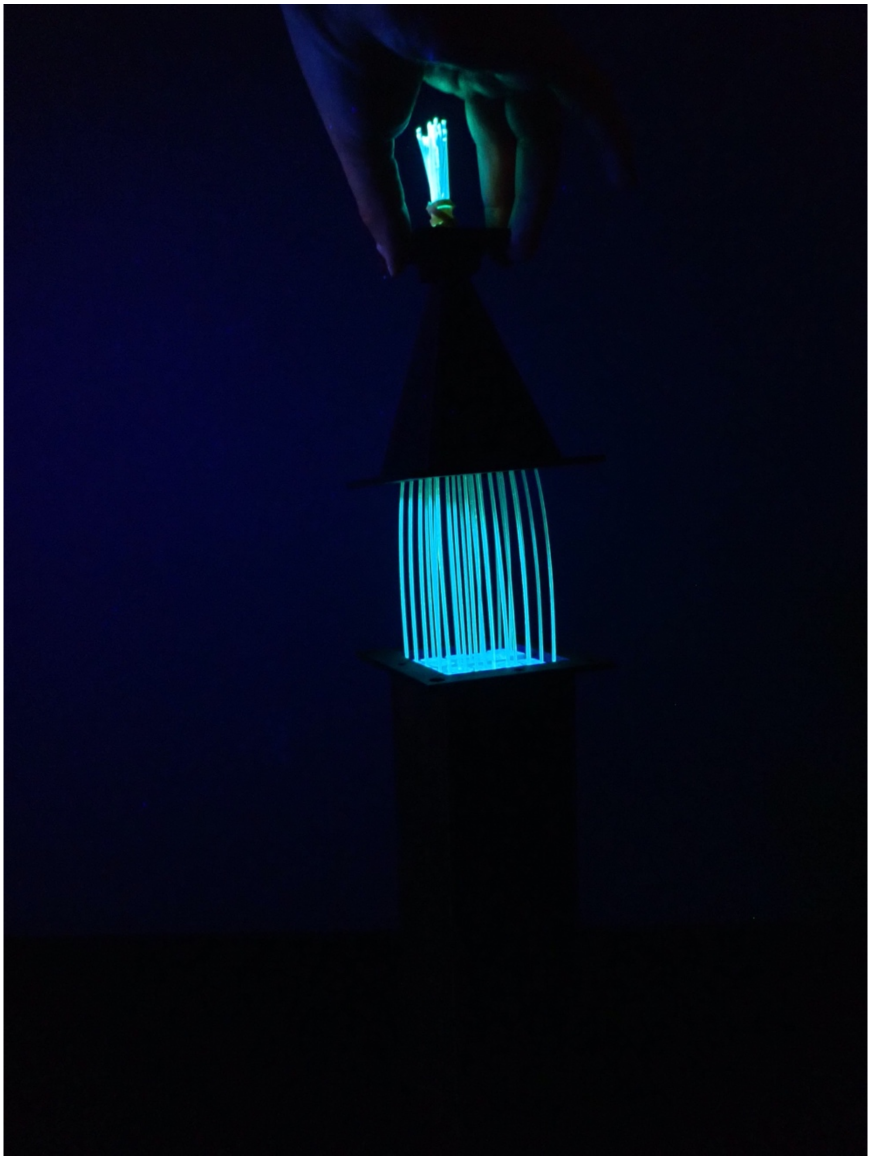

Figure 7: The photo shown here is identical to Figure 6 but under dark conditions and illuminated by a UV light.

Figure 8: Final assembly of one-pixel detector unit.

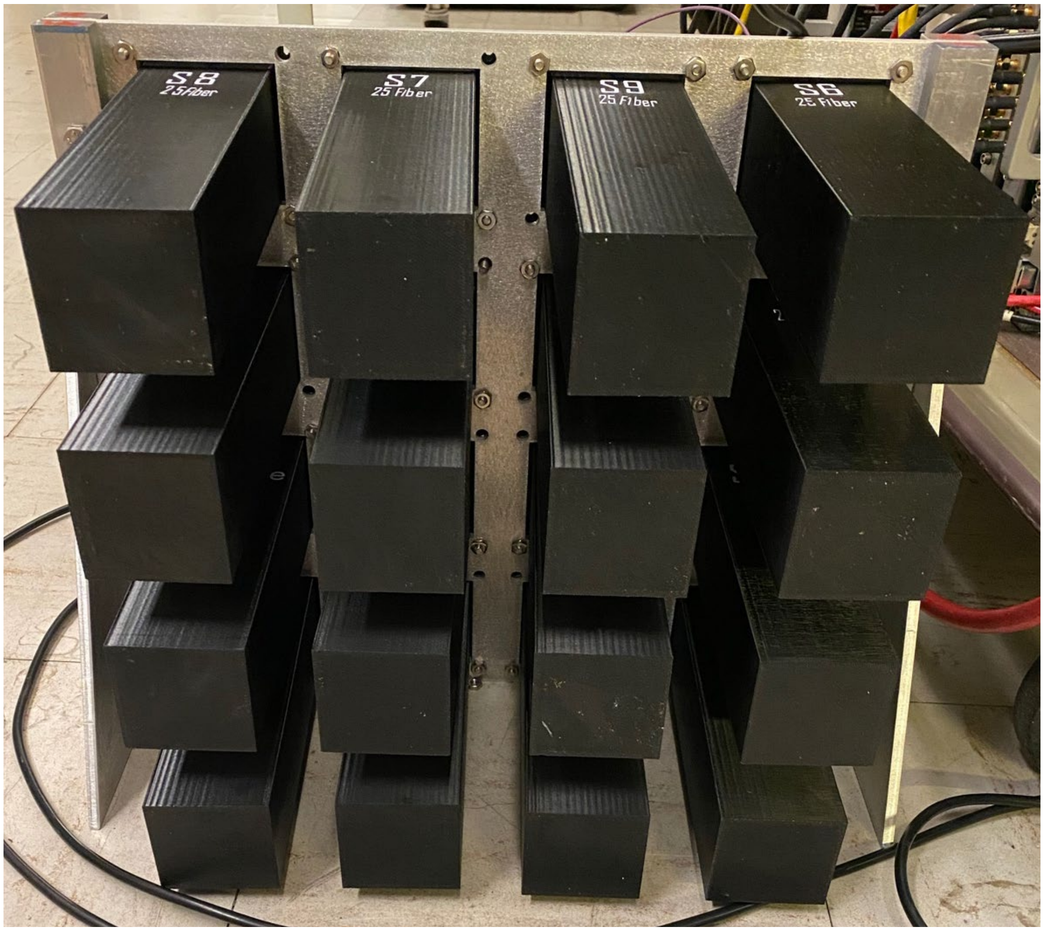

Figure 9: 4×4 array of detector units held in place by an aluminum frame.

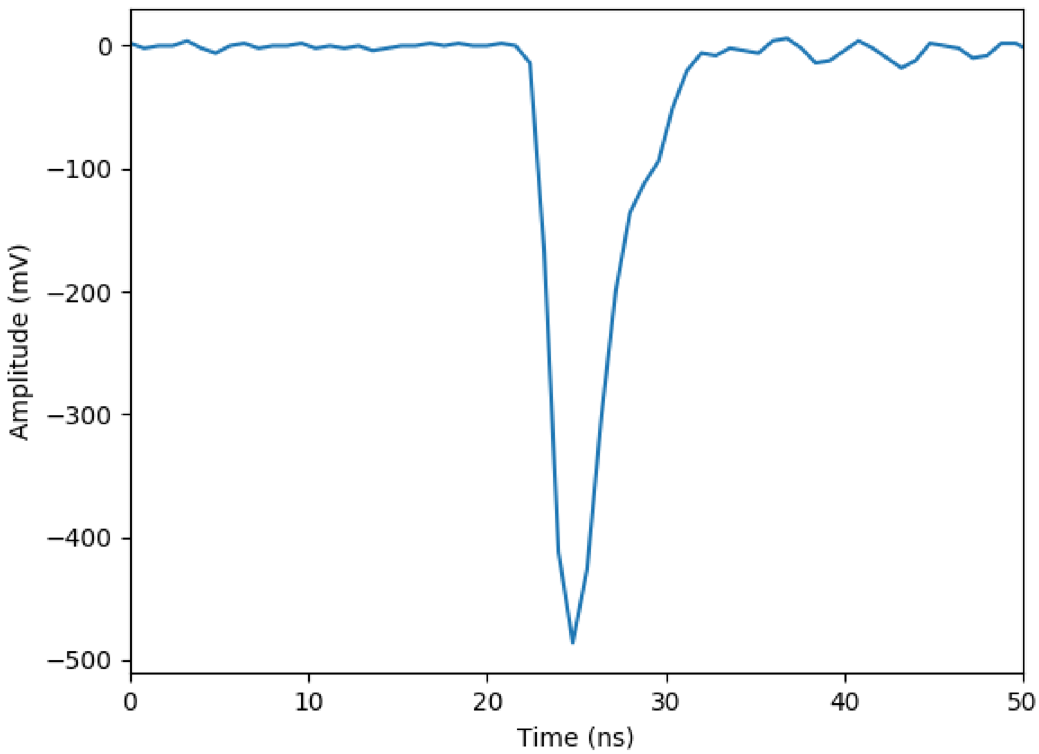

Figure 10: Representative pulse from the 25-fiber bundle array read out by the R9880U-01 PMT in response to a cosmic-ray muon.

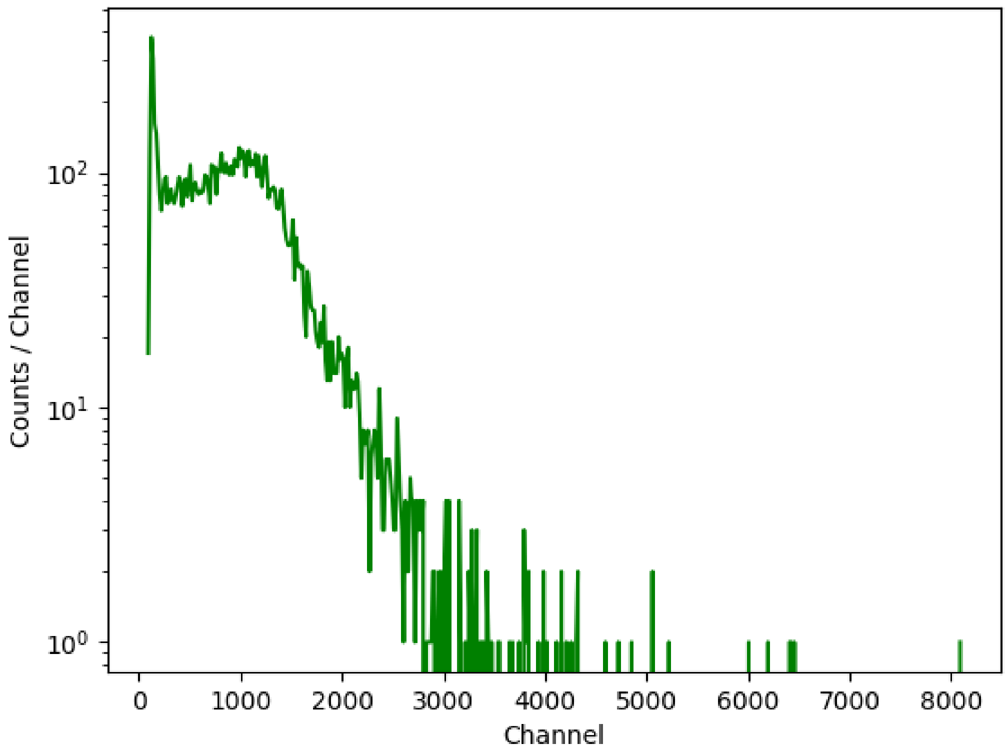

Figure 11: Muon spectrum as measured by a 25-fiber bundle array read out by a R9880U-01 PMT.

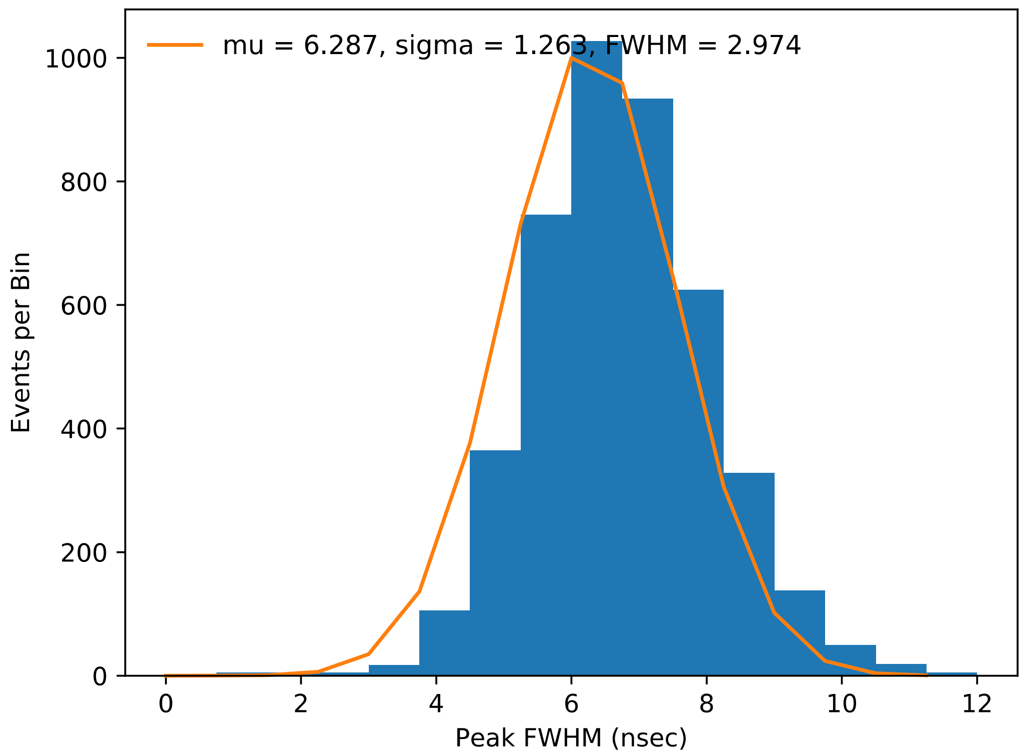

Figure 12: Timing distribution of the peak FWHM of PMT pulses for the cosmic-ray muon peak, achieving a mean of ~6 ns.

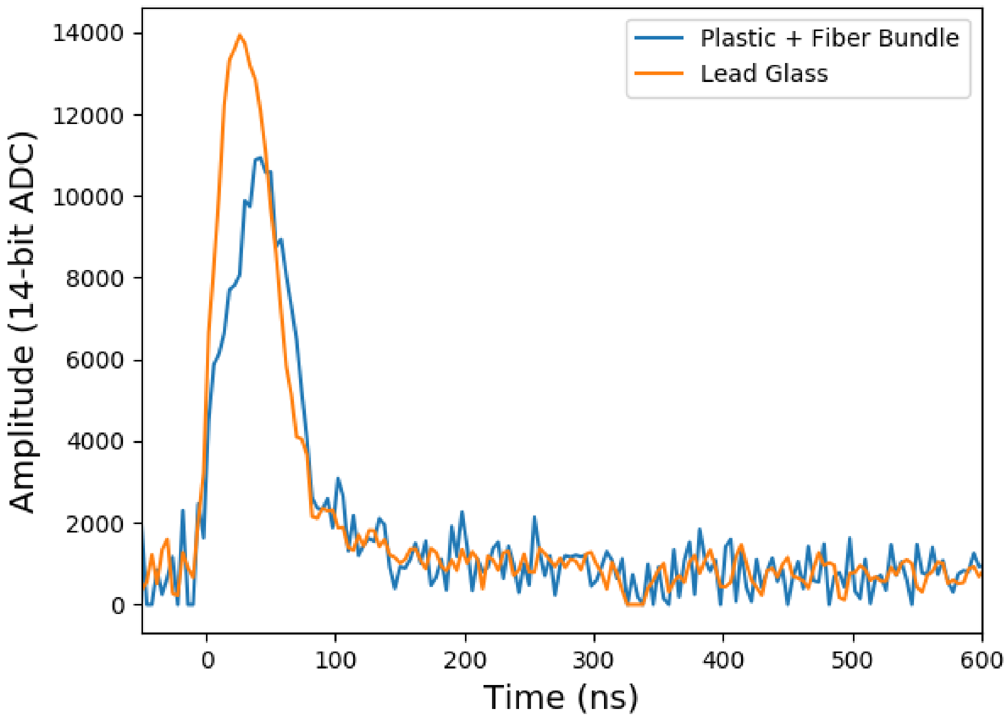

Figure 13: Signal measured by a fiber detector exposed to a pulse from the NRL Mercury pulsed-power facility, along with a signal from a lead-glass detector with known fast response to indicate that the width of the pulse is not due to instrument response time. Both detectors were read out by the SIS3316 fADCs (with 4 ns sampling rate).